

Afyon Kocatepe Üniversitesi Fen ve Mühendislik Bilimleri Dergisi

Afyon Kocatepe University - Journal of Science and Engineering

https://dergipark.org.tr/tr/pub/akufemubid



e-ISSN: 2149-3367 AKÜ FEMÜBİD 25 (2025) 051102 (1032-1039)

Araştırma Makalesi / Research Article DOI: https://doi.org/10.35414/akufemubid.1643029 AKU J. Sci. Eng. 25 (2025) 051102 (1032-1039)

> *Makale Bilgisi / Article Info Alındı/Received: 19.02.2025 Kabul/Accepted: 23.04.2025 Yayımlandı/Published: 01.10.2025

Structural, Vibrational, and Electronic Properties of 2,5-Bis(1-Naphthyl)-1,3,4-Oxadiazole: **Experimental and Theoretical Investigation**

2,5-Bis(1-Naftil)-1,3,4-Oksadiazole'nin Yapısal, Titreşimsel ve Elektronik Özellikleri: Deneysel ve Teorik Araştırma

Emine BABUR SAS^{1*} , Mustafa KURT²

¹Kirsehir Ahi Evran University, Technical Sciences Vocational School, Department of Electronics and Automation, Türkiye





© 2025 The Authors | Creative Commons Attribution-Noncommercial 4.0 (CC BY-NC) International License

Abstract

This study used both theoretical and experimental methods to examine the structural, vibrational, and electrical characteristics of the 2,5-Bis(1-naphthyl)-1,3,4-oxadiazole (BND) molecule. The vibrational wave numbers, bond lengths, and bond angles of the optimized molecular structure were examined and compared to the experimental results. Plots of the correlation between the recorded FT-IR and FT-Raman spectra and the Density Functional Theory (DFT) computations were created. Furthermore, chemical shift values were theoretically predicted using the GIAO method in THF solvent and NMR spectra were collected; these values demonstrated a satisfactory correlation with the experimental values. The frontier molecular orbitals (HOMO-LUMO) were analyzed to assess the electronic properties, and a sizable energy gap that demonstrated the molecule's stability was discovered. The charge distribution and active spots in the molecule were revealed by 2D contours and molecular electrostatic potential (MEP) surface analysis.

Keywords: DFT; FT-IR; FT-Raman; NMR; HOMO-LUMO; MEP.

2,5-Bis(1-naftil)-1,3,4-oksadiazol çalışmada, molekülünün yapısal, titreşim ve elektriksel özellikleri hem teorik hem de deneysel yöntemlerle incelenmiştir. Optimize edilmiş moleküler yapının titreşim dalga sayıları, bağ uzunlukları bağ açıları incelenmiş ve deneysel sonuçlarla karşılaştırılmıştır. Kaydedilen FT-IR ve FT-Raman spektrumları ile Yoğunluk Fonksiyonel Teorisi (DFT) hesaplamaları arasında korelasyon grafikleri oluşturulmuştur. Ayrıca, kimyasal kayma değerleri THF çözücüsünde GIAO yöntemi kullanılarak teorik olarak tahmin edilmiş ve NMR spektrumları toplanmıştır; bu değerler deneysel değerlerle tatmin edici bir korelasyon göstermiştir. Elektronik özellikleri değerlendirmek için sınır moleküler orbitalleri (HOMO-LUMO) analiz edilmiş ve molekülün kararlılığını gösteren önemli bir enerji boşluğu keşfedilmiştir. Moleküldeki yük dağılımı ve aktif noktalar 2D konturlar ve moleküler elektrostatik potansiyel (MEP) yüzey analizi ile ortaya çıkarılmıştır.

Anahtar Kelimeler: DFT; FT-IR; FT-Raman; NMR; HOMO-LUMO; MEP.

1. Introduction

Oxadiazole derivatives have attracted significant attention due to their wide range of applications in pharmaceuticals, materials science and corrosion inhibition (Bouklah et al. 2005, Fouda et al. 2006). These heterocyclic compounds exhibit unique electronic and structural properties that contribute to their biological activities, including antimicrobial, anti-inflammatory and anticancer effects (Holla et al. 2003, Foroumadi et al. 2003, Bajaj et al. 2015). Furthermore, oxadiazole-based molecules have been investigated for their ability to act as corrosion inhibitors by adsorbing onto metal surfaces and reducing material degradation (Lagrenee et al. 2001). The effectiveness of oxadiazole derivatives in corrosion inhibition is closely linked to their molecular structure and

electronic properties (El-Rehim et al. 1999) Organic inhibitors generally function by donating electrons to the metal surface, forming stable coordination bonds (Hosseini and Azimi 2009, Chebabe et al. 2003, Fuentealba et al. 2000).

A number of oxadiazoles with high electron transport potentials have been studied in the literature in materials science (Tokuhisa et al. 1995, Chang et al. 2015, Reig et al. 2017, Peng et al. 1998). Especially compounds with 1,3,4 oxadiazole rings are investigated for their optical and electronic properties for the fabrication of OLEDs (Yang et al. 2015, Tao et al. 2011, Hughes and Bryce, 2005). Anthracene derivatives of the molecule BND investigated in this paper have significant potential as electron transport layers (Reddy et al. 2011). The structure of organic compounds has a significant effect on the properties of materials, especially in solvent media (Krukiewicz et al. 2016, Huangzhong 2010, Jeon et al. 2013, Tanış et al. 2018).

Computational methods, especially Density Functional Theory (DFT), have proven to be powerful tools for studying the electronic structure and vibrational properties of oxadiazole derivatives (Andzelm and Wimmer 1992, Stephens et al. 1994). DFT calculations allow researchers to optimize molecular geometries, predict infrared (IR) and Raman spectra, and analyze electron density distribution (Fang and Li, 2002). By comparing theoretical results with experimental spectroscopic data, it is possible to obtain deeper insights into the structure-property relationships of these compounds (Rodríguez-Valdez et al. 2005, Şaş et al. 2022)

Using both experimental and theoretical methods, we examine the structural, vibrational, and electrical characteristics of the BND molecule in this work. Previously, we concentrated on its optical features (Sas et al. 2018). We examine the molecular structure of these molecules using DFT simulations in conjunction with infrared and Raman spectroscopy methods. The results of this study advance a more thorough comprehension of the uses of oxadiazole derivatives in both scientific and industrial domains.

2. Materials and Methods

A 97% pure powder sample of the 2,5-Bis(1-naphthyl)-1,3,4-oxadiazole molecule was provided by Across Organics. The molecule's FT-IR and FT-Raman spectra were captured between 4000-400 cm-1 and 3500-10 cm-1. Using the KBr disc method, the Perkin Elmer BX spectrometer's FT-IR spectrum was acquired. The Agilent brand 600 MHz frequency, 14.1 tesla field power Premium Compact NMR apparatus, and THF-dd solvent were used to record the 1H-NMR and 13C-NMR spectra using parts per million (ppm).

The Gaussian 09 software (Frisch et al. 2009) and the DFT / B3LYP / 6-311G ++ (d, p) base set (Hohenberg and Kohn, 1964, Becke 1992) were used for all of the calculations in this investigation. This basis set was used to optimize the molecule and determine its geometrical characteristics and vibrational frequencies. The estimated vibration frequencies were multiplied by the scaling factor from the particular references to get them closer to the experimental vibration frequencies. NMR studies and frontier molecular orbitals were also carried out for the BND molecule. 13C and 1H NMR chemical shifts were calculated in THF solvent using the GIAO method and the B3LYP/6-311G(d,p) basis set (Ditchfield 1972, Wolinski et

al. 1990). A 3D surface map displaying the molecule's electron density was used to visualize and analyze the molecular electrostatic potential surface (MEP).

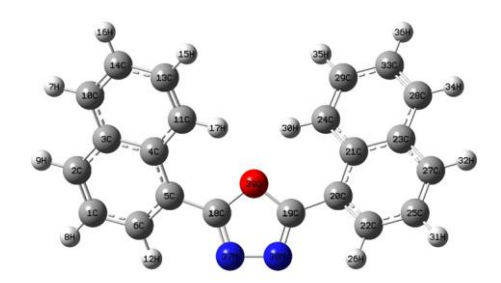


Figure 1. The BND's theoretically optimal geometric structure.

3. Results and Discussions

3.1 Structural and Vibrational Analysis

BND molecule is a molecule with an empirical formula C22H14N2O having two single bonds and thirty-nine atoms. The molecule is rotated around single bonds and the least energy structure has been found and optimized. Fig. 1 shows the molecule's optimal structure. Using the fundamental set of 6-311 ++ G (d, p), the values of the bond lengths and bond angles—the molecule's structural parameters—are computed and provided in Table 1.

Table 1. Some geometric parameters of the BND molecule [Bond Lengths (Å), Bond Angles (°)]

Bond	Bond Length		Bond Angles		
C1-C2	1.373	C2-C1-C6	119.9		
C1-C6	1.405	C2-C1-H8	120.6		
C1-H8	1.083	C6-C1-H8	119.4		
C3-C4	1.436	C1-C2-C3	120.8		
C5-C18	1.463	C1-C2-H9	120.6		
C6-H12	1.082	C3-C2-H9	118.6		
C10-C14	1.371	C2-C3-C4	119.9		
H7-C10	1.085	C2-C3-C10	120.6		
C11-H17	1.079	C4-C3-C10	119.5		
C13-H15	1.084	C3-C4-C5	117.8		
C14-H16	1.084	C3-C4-C11	117.7		
C24-H30	1.079	C5-C4-C11	124.5		
N37-N38	1.381	C4-C5-C6	119.9		
C18-N37	1.299	C4-C5-C18	124.5		
C18-O39	1.368	C6-C5-C18	115.6		
C19-N38	1.299	C1-C6-C5	121.5		
C19-O39	1.368	C1-C6-H12	120.2		

The BND molecule's C-C and C-H bond lengths at its lowest energy were determined to be between 1.3714 and 1.4634 Å and 1.0849 and 1.079 Å, respectively. The C-C-C bond angles were determined to be between 115.6 and 124.5 Å. The carbon atoms in the phenyl ring connected to the carbon atoms of the oxadiazole ring had bond lengths of 1.46 Å between 5C-18C and 19C-20C. It was determined that the C-C bond lengths at the oxadiazole ring were 1.43 Å. The molecule's C-H bond lengths are typically determined to be 1.08 Å. However, because of intramolecular contact, the C11-H17 and C24-

H30 bond lengths were determined to be 1.079 Å. The BND molecule next to the oxadiazole ring has C-C-C bond angles of 117 degrees, whereas the phenyl ring has C-C-C bond angles of 120 degrees.

Although the BND molecule's structure parameters have been compared to those of related compounds, the molecule's crystal structure has not yet been identified in the literature.

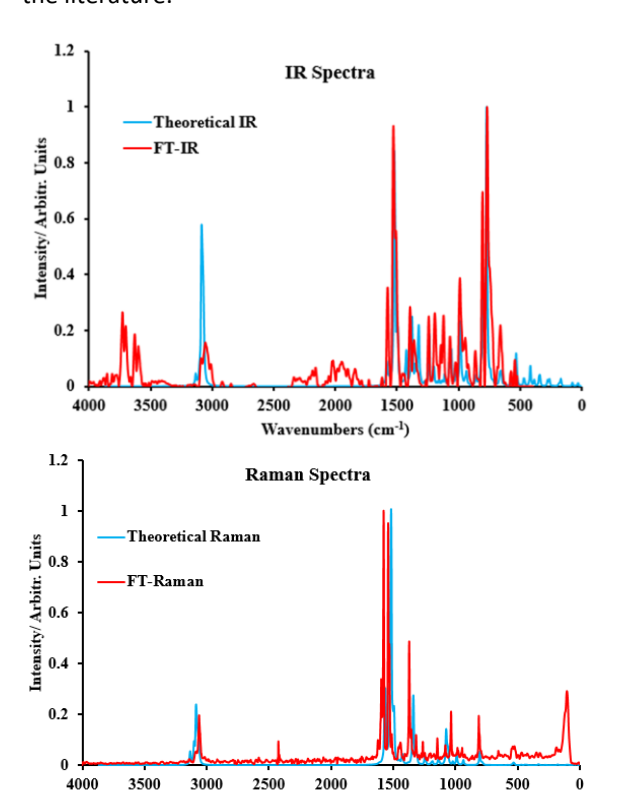


Figure 2. The BND's FT-IR and FT-Raman spectra, both experimentally and computationally (using the scaling factor).

Wavenumbers (cm⁻¹)

In the 1,3,4 oxadiazole molecule, the C=N bond was calculated as 1.291 Å, the N-N bond was 1.405 Å, and the C-O bond was 1.360 Å (El-Azhary 1996). In the 5-phenyl-1,3,4-oxadiazole-2-thiol molecule, E Romana et al. calculated the same bond lengths as 1.293 Å, 1.396 Å and 1.357 Å, respectively (Romano et al. 2012) This molecule also has a phenyl ring attached to the oxadiazole ring and the C-C bond length which provides this linkage is calculated to be 1.457 Å (Romano et al. 2012).

According to the X-Ray data of the 5-phenyl-1,3,4-oxadiazole-2-thiol molecule, the same bonds were 1.285 Å, 1.376 Å, 1.367 Å and 1.454 Å, respectively (Singh et al. 2007). C=N, N-N and C-O bonds in the studied molecule were found to be 1.299, 1.381, 1.368, respectively.

BND molecule 111 (3N-6) has fundamental vibration. Wavenumbers are calculated according to the minimum energy situation. The estimated wavenumbers were multiplied by scaling factors 0.967 (int. ref. 1) to match the experimental values. The experimental and

theoretical vibration spectra are shown on a single graph in Figs. 2 and 3 for comparison.

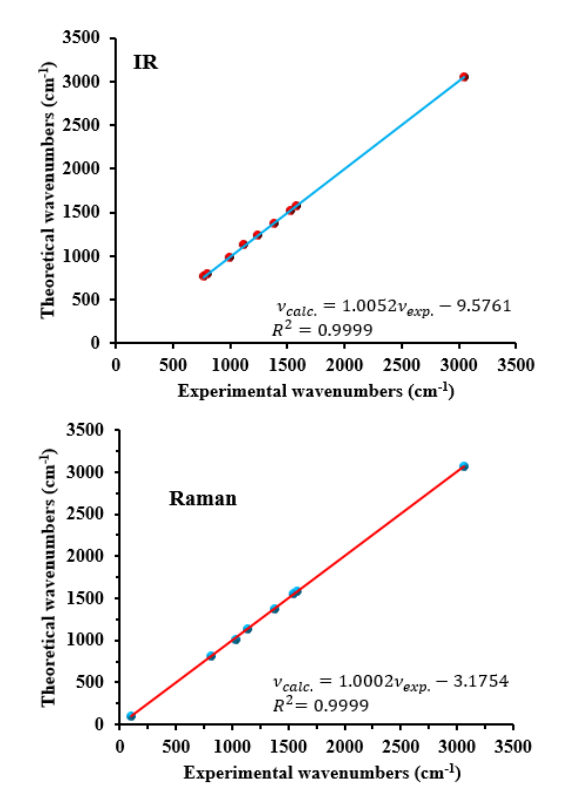


Figure 3. The BND's computed and experimental correlation graph

In the theoretical Raman spectrum, the sharpest band are seen at 1517 cm-1 with the scaling factor. This vibrational mode is the band in which the C=N stretching vibration. This value corresponds to 1579 cm-1 in the experimental Raman spectrum. This peak is seen as the sharpest peak in the experimental IR spectrum (1529 cm-1). However, the theoretical IR was assigned as the second sharpest peak (1523 cm-1) in the spectrum. C-N stretching band is a mixed band with CCH bending or C-C stretching vibration. Of the 111 basic vibration bands of the BND molecule, 14 were named pure bands and this band was assigned as the C-H band. C-H vibration band was calculated in the range of 3132-3057 cm-1. This band in FT-Raman was also observed at 3061 cm-1, while FT-IR was observed at 3048 cm-1. Theoretical and experimental wavenumbers are compared in Table 2.

C-C and C=C vibration bands in ring usually recorded in range of 1430–1625 cm-1 (Krishnakumar and Xavier 2003, Singh and Yadav 2001). These bands by Varsanyi are observed in between of 1625–1561, 1575–1590, 1470–1540, 1430–1465 and 1280–1380 cm-1 (Varsányi 2012). These vibrations of BND molecule intensely were computed at 1608-1491, 1333-1340, 1269-1306, 1196, 1015-1054 cm-1 and observed at 1529, 1577 cm-1 and at 1541, 1579, 1032 cm-1 in FT-IR and FT-Raman, respectively.

Table 2. Some computed and observed vibrational spectra of the BND molecule are compared.

	FT-IR	FT-Raman	freq	scaled	I _{IR}	S_{RA}
6		101	107	103	0.1	4.9
37	764		791	765	9.9	4.6
43	803		825	798	0.6	183.3
44		815	841	813	6.1	5.5
58	997		1017	984	0.8	156.5
60		1032	1050	1015	1.6	5.2
65	1120		1166	1128	2.4	51.8
67		1140	1173	1134	0.4	37.4
75	1241		1283	1241	0.1	109.1
83	1387	1379	1423	1376	8.5	2.8
91	1529		1569	1517	90.9	238.6
92		1541	1614	1561	1.1	1300.4
94	1577		1632	1578	12.8	5.5
95		1579	1634	1580	1.1	6.1
98	3048		3162	3057	0.8	9.2
100		3061	3166	3062	1.5	59.7
110			3239	3132	1.9	4.3
111			3240	3133	2.9	185.5

Table 3. Some chemical changes (ppm) of BND, both theoretical and experimental

Atom	Theor	etical	Experimental
	THF	Gas	THF
C19	180.81	179.39	164.05
C18	180.68	179.24	164.05
C2	138.29	136.61	133.99
C6	134.97	134.54	129.84
C4	133.27	133.73	128.59
C13	132.45	131.26	127.17
C33	131.28	130.35	125.95
C1	129.94	129.58	120.14
C5	124.53	126.21	120.14
H30	9.23	9.20	9.27
H17	9.17	9.14	9.27
Н9	8.51	8.26	8.43
H26	8.46	8.4	8.25
H7	8.38	8.17	8.23
H15	8.23	8.02	8.10
H16	8.00	7.81	7.79
Н8	7.99	7.82	7.74

3.2 NMR Analysis

Aromatic protons and carbons generally give signals with chemical shift values between 7-8 ppm and 100-150 ppm, respectively (Kalinowski 1988)

All aromatic carbon atoms' chemical shift values, with the exception of C18 and C19 atoms, were computed within this range based on the values listed in Table 3. Examining the chemical shift values of the theoretical and experimental data in THF solvent reveals that the results are in agreement. The oxadiazole ring's C18 and C19 atoms' chemical shift value was measured at 164 ppm and computed to be 180 ppm.

When the aromatic protons of BND molecule were examined, they were observed in the range 7-8 except H17 and H30 atoms which are close to the oxygen atom in the oxadiazole ring and were calculated in this range

theoretically. Figure 4 shows the BND molecule's 13C and 1H NMR spectra obtained in THF solvent. The shielding of electronegative atoms may be the reason why the chemical shift values of H17 and H30 atoms do not fall within this range. The relationship between experimental chemical shift values and calculated chemical shift values (correlation graph) is given in Figure 4. According to the correlation graph, the theoretical and experimental values are in agreement.

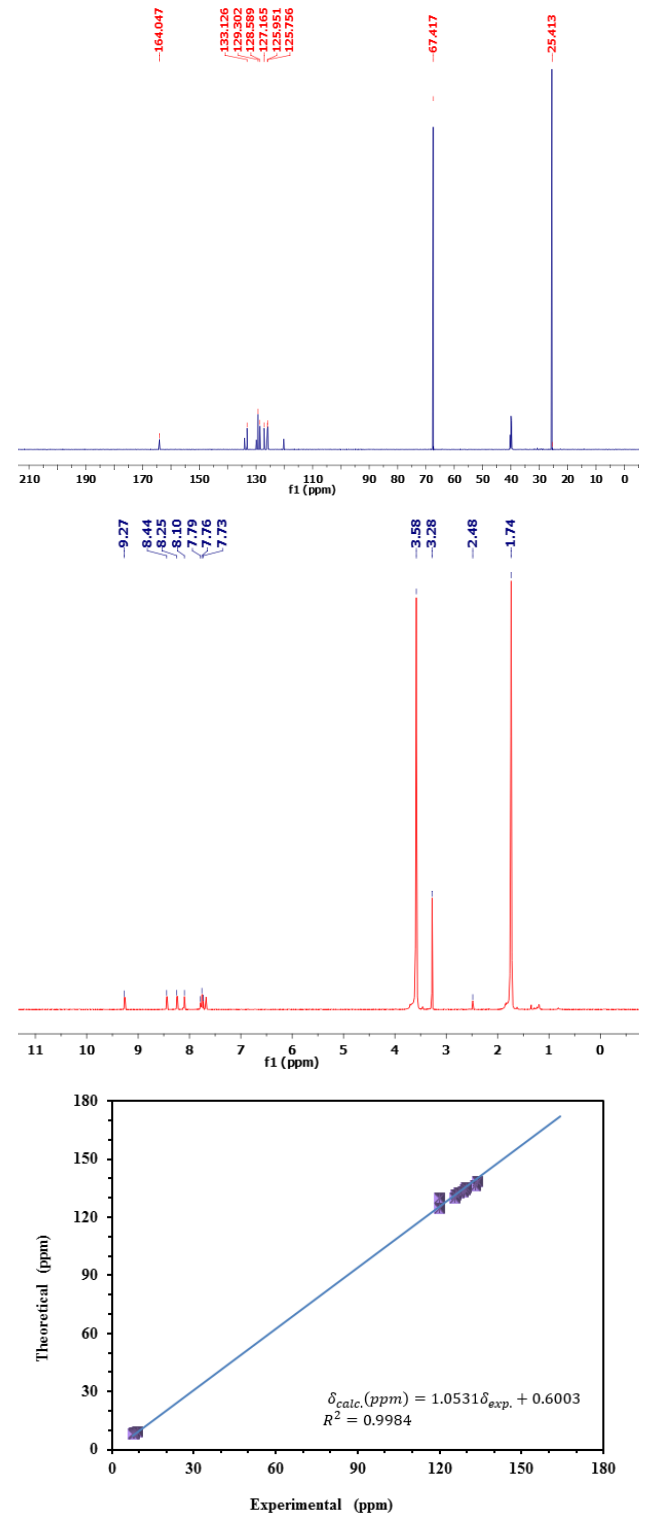


Figure 4. The BND in THF solution's 1 H and 13 C NMR spectra and correlation graph.

3.3 Frontier Molecular Orbitals Analysis

One crucial factor affecting electron conductivity is the energy differential between the HOMO and LUMO energy levels (Fleming, 1976). The molecule's chemical stability and the charge transfer that occurs within it are also explained by the energy gap. In essence, the energy gap establishes how much energy is needed for the molecule to change from its most stable ground state to an excited state.

The HOMO energy level of the BND molecule in the gas phase is -6.20 eV, its LUMO energy level is -1.97 eV, and its HOMO-LUMO energy differential is 4.23 eV, based on calculations. The THF solvent and gas phase energy values are shown in Table 4.

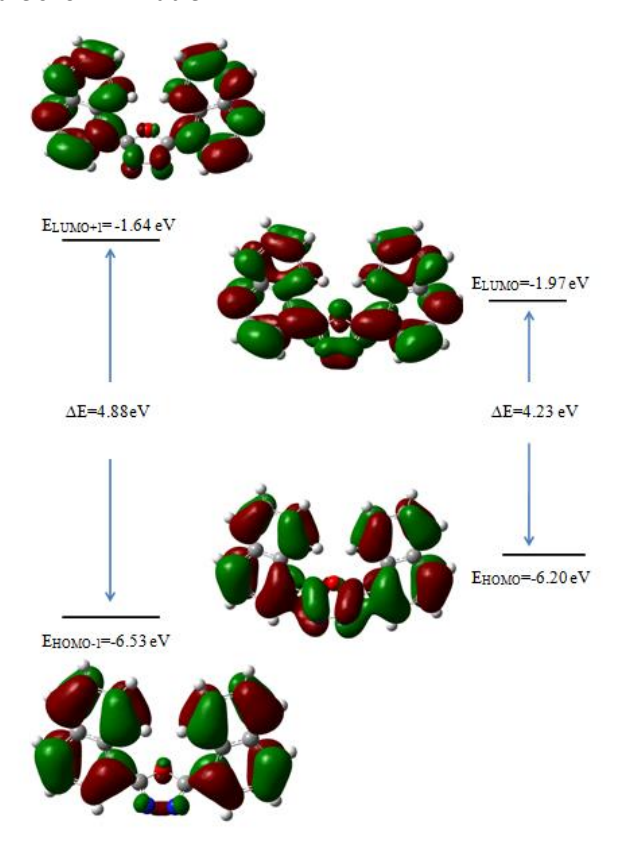


Figure 5. The BND's gas phase frontier molecular orbitals.

Table 4. Determined energy values and a few BND parameters

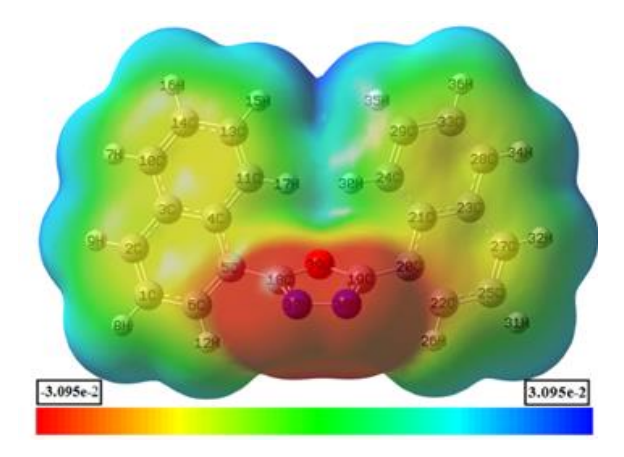
Parameters	GAS	THF
E _{total} (Hartree)	-1031.6	-1031.4
E _{HOMO} (eV)	-6.20	-6.05
E _{LUMO} (eV)	-1.97	-1.79
E _{HOMO-1} (eV)	-6.53	-6.32
E _{LUMO+1} (eV)	-1.64	-1.42
E _{HOMO-1-LUMO+1 gap} (eV)	4.89	4.26
E _{номо-LUMO gap} (eV)	4.23	4.90
Chemical hardness (h)	2.12	2.45
Electronegativity (χ)	4.09	3.92
Chemical potential (μ)	-4.09	-3.92

The initial nearby molecular orbitals are analyzed and plotted in the gas phase, as seen in Figure 5, to provide a

more detailed view of the energy level differences. The positive phase in this graph is represented by the color red, while the negative phase is represented by the color green. The charge density of the LUMO orbitals is localized throughout the entire structure, with the exception of the H atoms, whereas the charge density of the HOMO orbitals is concentrated in all rings of the molecule save the H and O atoms. The values for the molecule's chemical hardness, electronegativity, and electrophilic index were also computed and are displayed in the table.

3.4 Molecular Electrostatic Potential Surface

Estimating the interplay of various geometries is made possible by the 2D contour map (Scrocco and Tomasi 1978, Politzer et al. 1985, Munoz-Caro et al 2000). Figure 6 shows the BND molecule's electrostatic potential surface (MEP) as a 2D contour and 3D surface. For the data on the 3D electrostatic potential surface, every color in this spectrum—from red to blue—was utilized.



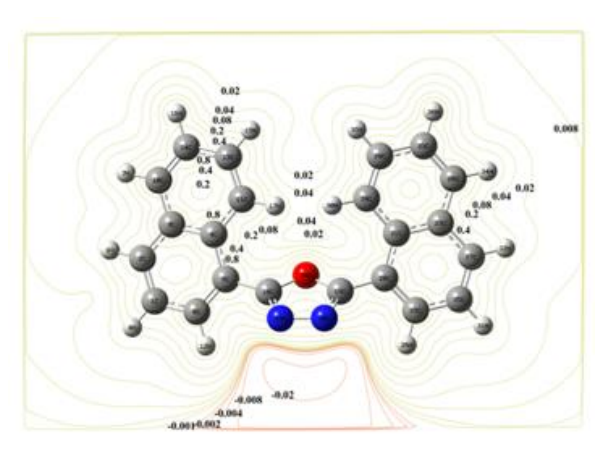


Figure 6. 3D and 2D contour maps of molecular electrostatic potential (MEPs) for BND.

For the molecule, these hues range from -3.095 a.u. (dark red) to 3.095 a.u. (dark blue). Electron-withdrawing events are indicated by blue hues, while electron-repulsive reactions are indicated by red hues. The molecule's negative potential is located around the N and

O atoms, while the positive potential is located close to the H atoms. These findings indicate that N and O atoms have strong repulsive reactions and H atoms have strong electron-withdrawing reactions. The molecular plane displays the BND molecule's 2D outline. The lines surrounding the hydrogen atoms show that they are electron-poor, while the values surrounding the oxygen and nitrogen atoms show that they are electron-rich. Nucleophilic and electrophilic regions are represented by negative and positive values, respectively. Around N atoms, a value of -0.02 a.u. is seen, but the molecule's center shows a value of 0.2.

4. Conclusions

This study used both theoretical and experimental methods to investigate the structural, vibrational, and electrical properties of the 2,5-Bis(1-naphthyl)-1,3,4-oxadiazole (BND) molecule. The molecule's ideal structure was contrasted with similar compounds that had bond lengths and angles determined. The real results obtained by FT-IR and FT-Raman spectroscopy were found to be in good agreement with the theoretical vibrational frequencies that were calculated and scaled using the DFT technique.

In the NMR investigation, there was a significant correlation between the experimental data and the chemical shift values that were calculated theoretically. We used equations based on the HOMO-LUMO energy difference or sum to determine the molecule's electronic properties, which included chemical hardness, chemical potential, and electrophilicity. The molecular electrostatic potential (MEP) map analysis helped identify potential electrophilic and nucleophilic spots by showing the electron density distribution throughout the molecule.

In conclusion, experimental and theoretical studies have revealed the vibrational and electronic properties of the BND molecule. The obtained results show that BND may be a potential candidate in electronic and optoelectronic applications.

Declaration of Ethical Standards

This article is a partially modified and improved version of the paper titled "Detailed Spectroscopic Analysis and Geometric Optimization of 2,5-Bis(1-naphthyl)-1,3,4-oxadiazole" which was presented orally at the (International Trace Analysis Congress (iTAC 2018), Sivas/Turkey, 20-23 June 2018) Congress but the full text was not published.

The authors declare that they comply with all ethical standards.

Credit Authorship Contribution Statement

Author-1: Conceptualization, investigation, methodology and software, visualization and writing – original draft.

Author-2: Research, Opinionator, Experimental design, Project Manager, Visualization, Writing – original draft

Declaration of Competing Interest

The authors declare that they have no known competing financial interests or personal relationships that could have appeared to influence the work reported in this paper.

The authors have no conflicts of interest to declare regarding the content of this article.

Data Availability Statement

All data generated or analyzed during this study are included in this published article.

Acknowledgement

This research was supported by the Ahi Evran University Scientific Research Projects Coordination (Project No: PYO-FEN.4001.14.009).

5. References

Andzelm, J., & Wimmer, E. 1992. Density functional Gaussian-type-orbital approach to molecular geometries, vibrations, and reaction energies. *The Journal of chemical physics*, *96*(2), 1280-1303. https://doi.org/10.1063/1.462165

Bajaj, S., Asati, V., Singh, J., & Roy, P. P., 2015. 1, 3, 4-Oxadiazoles: An emerging scaffold to target growth factors, enzymes and kinases as anticancer agents. *European journal of medicinal chemistry*, **97**, 124-141. https://doi.org/10.1016/j.ejmech.2015.04.051

Becke, A. D. 1992. Density-functional thermochemistry. I. The effect of the exchange-only gradient correction. *The Journal of chemical physics*, *96*(3), 2155-2160. https://doi.org/10.1063/1.462066

Bouklah, M., Hammouti, B., Benkaddour, M., & Benhadda, T., 2005. Thiophene derivatives as effective inhibitors for the corrosion of steel in 0.5 m H2 SO4. *Journal of Applied Electrochemistry*, **35**, 1095-1101.

https://doi.org/10.1007/s10800-005-9004-z

Chang, C. H., Griniene, R., Su, Y. D., Yeh, C. C., Kao, H. C., Grazulevicius, J. V., ... & Grigalevicius, S. 2015. Efficient red phosphorescent OLEDs employing carbazolebased materials as the emitting host. *Dyes and Pigments*, **122**, 257-263.

https://doi.org/10.1016/j.dyepig.2015.06.038

Chebabe, D., Chikh, Z. A., Hajjaji, N., Srhiri, A., & Zucchi, F., 2003. Corrosion inhibition of Armco iron in 1 M HCl solution by alkyltriazoles. *Corrosion science*, *45*(2), 309-320.

https://doi.org/10.1016/S0010-938X(02)00098-7

Ditchfield, R. 1972. Molecular orbital theory of magnetic shielding and magnetic susceptibility. *The Journal of Chemical Physics*, *56*(11), 5688-5691. https://doi.org/10.1063/1.1677088

El-Azhary, A. A. 1996. Vibrational analysis of the spectra of 1, 3, 4-oxadiazole, 1, 3, 4-thiadiazole, 1, 2, 5-oxadiazole and 1, 2, 5-thiadiazole: comparison

- between DFT, MP2 and HF force fields. *Spectrochimica Acta Part A: Molecular and Biomolecular Spectroscopy*, **52(1)**, 33-44.
- https://doi.org/10.1016/0584-8539(95)01535-3
- El-Rehim, S. A., Ibrahim, M. A., & Khaled, K. F., 1999. 4-Aminoantipyrine as an inhibitor of mild steel corrosion in HCl solution. Journal of Applied Electrochemistry, 29, 593-599.
 - https://doi.org/10.1023/A:1003450818083
- Fang, J., & Li, J. 2002. Quantum chemistry study on the relationship between molecular structure and corrosion inhibition efficiency of amides. *Journal of Molecular Structure: THEOCHEM*, **593(1-3)**, 179-185. https://doi.org/10.1016/S0166-1280(02)00316-0
- Fleming I., 1976. Frontier Orbitals and Organic Chemical Reactions, Wiley, London.
- Fouda, A. S., Al-Sarawy, A. A., & El-Katori, E. E., 2006. Pyrazolone derivatives as corrosion inhibitors for C-steel in hydrochloric acid solution. *Desalination*, **201(1-3)**, 1-13.
 - https://doi.org/10.1016/j.desal.2006.03.519
- Foroumadi, A., Mansouri, S., Kiani, Z., & Rahmani, A., 2003. Synthesis and in vitro antibacterial evaluation of N-[5-(5-nitro-2-thienyl)-1, 3, 4-thiadiazole-2-yl] piperazinyl quinolones. *European journal of medicinal chemistry*, **38**(9), 851-854. https://doi.org/10.1016/S0223-5234(03)00148-X
- Frisch, M. J. E. A., Trucks, G. W., Schlegel, H. B., Scuseria, G. E., Robb, M. A., Cheeseman, J. R., ... & Fox, D. J. 2009. gaussian 09, Gaussian. *Inc., Wallingford CT*, 121, 150-166.
- Hohenberg, P., & Kohn, W. 1964. Inhomogeneous electron gas. *Physical review*, **136(3B)**, B864. https://doi.org/10.1103/PhysRev.136.B864
- Fuentealba, P., Pérez, P., & Contreras, R. 2000. On the condensed Fukui function. *The Journal of Chemical Physics*, **113(7)**, 2544-2551. https://doi.org/10.1063/1.1305879
- Holla, B. S., Veerendra, B., Shivananda, M. K., & Poojary, B., 2003. Synthesis characterization and anticancer activity studies on some Mannich bases derived from 1, 2, 4-triazoles. *European Journal of Medicinal Chemistry*, 38(7-8), 759-767. https://doi.org/10.1016/S0223-5234(03)00128-4
- Hosseini, S. M. A., & Azimi, A., 2009. The inhibition of mild steel corrosion in acidic medium by 1-methyl-3-pyridin-2-yl-thiourea. *Corrosion Science*, *51*(4), 728-732.
 - https://doi.org/10.1016/j.corsci.2008.11.019
- Huangzhong, Y. 2010. Different solvents effect on the performance of the solar cells based on poly (3-hexylthiophene):methanofullerenes. *Synthetic Metals*, **160(23-24)**, 2505-2509. https://doi.org/10.1016/j.synthmet.2010.09.035

- Hughes, G., & Bryce, M. R. 2005. Electron-transporting materials for organic electroluminescent and electrophosphorescent devices. *Journal of Materials Chemistry*, **15(1)**, 94-107 https://doi.org/10.1039/B413249C
- Jeon, B. C., Kim, M. S., Cho, M. J., Choi, D. H., Ahn, K. S., & Kim, J. H. 2014. Effect of solvent on dye-adsorption process and photovoltaic properties of dendritic organic dye on TiO2 electrode of dye-sensitized solar cells. *Synthetic metals*, 88, 130-135. https://doi.org/10.1016/j.synthmet.2013.12.006
- Kalinowski, H. O., Berger, S., & Braun, S. 1988. Carbon-13 NMR spectroscopy. John Wiley and Sons, New York.
- Krishnakumar, V., & Xavier, R. J. 2003. Normal coordinate analysis of vibrational spectra of 2-methylindoline and 5-hydroxyindane. Indian Journal of Pure & Applied Physics, **41**, 95-99.
- Krukiewicz, K., Jarosz, T., Herman, A. P., Turczyn, R., Boncel, S., & Zak, J. K. 2016. The effect of solvent on the synthesis and physicochemical properties of poly (3, 4-ethylenedioxypyrrole). *Synthetic Metals*, *217*, 231-236.
 - https://doi.org/10.1016/j.synthmet.2016.04.005
- Lagrenee, M., Mernari, B., Chaibi, N., Traisnel, M., Vezin, H., & Bentiss, F., 2001. Investigation of the inhibitive effect of substituted oxadiazoles on the corrosion of mild steel in HCl medium. *Corrosion science*, 43(5), 951-962.
 - https://doi.org/10.1016/S0010-938X(00)00076-7
- Munoz-Caro, C., Nino, A., Senent, M. L., Leal, J. M., & Ibeas, S. 2000. Modeling of protonation processes in acetohydroxamic acid. *The Journal of organic chemistry*, *65*(2), 405-410. https://doi.org/10.1021/jo991251x
- Peng, Z., Bao, Z., & Galvin, M. E. 1998. Oxadiazole-Containing Conjugated Polymers for Light-Emitting Diodes. *Advanced Materials*, *10*(9), 680-684. https://doi.org/10.1002/(SICI)1521-4095(199806)10:9<680::AID-ADMA680>3.0.CO;2-H
- Politzer, P., Laurence, P. R., & Jayasuriya, K. 1985. Molecular electrostatic potentials: an effective tool for the elucidation of biochemical phenomena. *Environmental health perspectives*, *61*, 191-202. https://doi.org/10.1289/ehp.8561191
- Reddy, M. A., Mallesham, G., Thomas, A., Srinivas, K., Rao, V. J., Bhanuprakash, K., ... & Srivastava, R. 2011. Synthesis and characterization of novel 2, 5-diphenyl-1, 3, 4-oxadiazole derivatives of anthracene and its application as electron transporting blue emitters in OLEDs. Synthetic metals, 161(9-10), 869-880. https://doi.org/10.1016/j.synthmet.2011.02.015
- Reig, M., Gozálvez, C., Bujaldón, R., Bagdziunas, G., Ivaniuk, K., Kostiv, N., ... & Velasco, D. 2017. Easy accessible blue luminescent carbazole-based

- materials for organic light-emitting diodes. *Dyes and Pigments*, **137**, 24-35.
- https://doi.org/10.1016/j.dyepig.2016.09.062
- Rodríguez-Valdez, L. M., Martínez-Villafañe, A., & Glossman-Mitnik, D. 2005. CHIH-DFT theoretical study of isomeric thiatriazoles and their potential activity as corrosion inhibitors. *Journal of Molecular Structure: THEOCHEM*, **716**(1-3), 61-65.
 - https://doi.org/10.1016/j.theochem.2004.10.082
- Romano, E., Soria, N. A. J., Rudyk, R., & Brandán, S. A. 2012. Theoretical study of the infrared spectrum of 5-phenyl-1, 3, 4-oxadiazole-2-thiol by using DFT calculations. *Molecular Simulation*, *38*(7), 561-566. https://doi.org/10.1080/08927022.2011.640936
- Sas, E. B., Kurban, M., Gündüz, B., & Kurt, M. 2018. Photophysical, spectroscopic properties and electronic structure of BND: Experiment and theory. *Synthetic Metals*, *246*, 39-44. https://doi.org/10.1016/j.synthmet.2018.09.013
- Scrocco, E., & Tomasi, J. 1978. Electronic molecular structure, reactivity and intermolecular forces: an euristic interpretation by means of electrostatic molecular potentials. In *Advances in quantum chemistry*, Vol. 11, pp. 115-193, Academic Press. https://doi.org/10.1016/S0065-3276(08)60236-1
- Singh, N. P., & Yadav, R. A. 2001. Vibrational studies of trifluoromethyl benzene derivatives 1: 2-amino, 5-chloro and 2-amino, 5-bromo benzotrifluorides. *Indian Journal of Physics*, **75**, 347-355.
- Singh, N. K., Butcher, R. J., Tripathi, P., Srivastava, A. K., & Bharty, M. K. 2007. 5-Phenyl-1, 3, 4-oxadiazole-2 (3H)-thione. *Acta Crystallographica Section E: Structure Reports Online*, *63*(2), o782-o784. https://doi.org/10.1107/S1600536806052238
- Stephens, P. J., Devlin, F. J., Chabalowski, C. F., & Frisch, M. J. 1994. Ab initio calculation of vibrational absorption and circular dichroism spectra using density functional force fields. *The Journal of physical chemistry*, 98(45), 11623-11627. https://doi.org/10.1021/j100096a001
- Şaş, E. B., Çifçi, S., & Kurt, M. 2022. Spectroscopic Characterization and DFT Calculations on 1Hbenzimidazole-2-carboxylic acid monohydrate Molecule. Sakarya University Journal of Science, 26(5), 879-891. https://doi.org/10.16984/saufenbilder.1100391
- Tanış, E., Babur Sas, E., Gündüz, B., & Kurt, M. 2018. Required theoretical and experimental physical characteristics of tris [4-(diethylamino) phenyl] amine organic material. *Journal of Materials Science: Materials in Electronics*, 29, 16111-16119. https://doi.org/10.1007/s10854-018-9700-1
- Tao, Y., Yang, C., & Qin, J. 2011. Organic host materials for phosphorescent organic light-emitting diodes. *Chemical Society Reviews*, **40**(5), 2943-2970.

- https://doi.org/10.1039/C0CS00160K
- Tokuhisa, H., Era, M., Tsutsui, T., & Saito, S. 1995. Electron drift mobility of oxadiazole derivatives doped in polycarbonate. *Applied physics letters*, *66*(25), 3433-3435.
 - https://doi.org/10.1063/1.113378
- Varsányi, G. 2012. Vibrational spectra of benzene derivatives. Elsevier.
- Wolinski, K., Hinton, J. F., & Pulay, P. 1990. Efficient implementation of the gauge-independent atomic orbital method for NMR chemical shift calculations. *Journal of the American Chemical Society*, **112(23)**, 8251-8260.
 - https://doi.org/10.1021/ja00179a005
- Yang, X., Xu, X., & Zhou, G. 2015. Recent advances of the emitters for high performance deep-blue organic light-emitting diodes. *Journal of Materials Chemistry C*, **3(5)**, 913-944.
 - https://doi.org/10.1039/C4TC02474E

Internet References

1-https://cccbdb.nist.gov/vibscalejustx.asp (13.02.2025)